The Reaction of C_6H_5 with CO: Kinetic Measurement and Theoretical Correlation with the Reverse Process

Gi-Jung Nam, Wensheng Xia,† J. Park, and M. C. Lin*

Department of Chemistry, Emory University, Atlanta, Georgia 30322

Received: September 13, 1999; In Final Form: December 1, 1999

The kinetics of the C_6H_5 reaction with CO has been studied by the cavity ring-down spectrometric technique in the temperature range 295−500 K at 12−120 Torr pressure with Ar as the carrier gas. The reaction occurred near the high-pressure limit under the conditions used. A weighted least-squares analysis of all data gives the rate constant for the association reaction, $k_1 = 10^{11.93\pm0.14}\exp[-(1507 \pm 109)/T]$ cm^3 mole^{-1} s^{-1}), where the errors represent two standard deviations. Our result can correlated satisfactorily with the kinetic data reported by Solly and Benson for the reverse process (*J. Am. Chem. Soc*. **1971**, *93*, 2171) with the Rice−Ramsperger−Kassel−Marcus (RRKM) theory using the transition-state parameters computed quantum mechanically by the MP2 method with the 6-31G(d,p) basis set. Combination of the forward and reverse reaction data gives $\Delta H_1^\circ = -24.6 \pm 0.8$ kcal/mol at 0 K and $k_1^\infty = 5.3 \times 10^{14}\exp(-14\,600/T)$ s^{-1} for the temperature range 300−670 K. The heat of reaction, combining with the known heats of formation of the reactants, leads to $\Delta_f H_0^\circ$ (C_6H_5CO) = 32.5 ± 1.5 kcal/mol.

Introduction

Phenyl radicals play a pivotal role in the combustion of gasoline in which small aromatic hydrocarbons (benzene, toluene, and xylenes) are added as antiknock agents (up to 30%).[1] The C_6H_5 radical is also believed to be involved in the formation of polycyclic aromatic hydrocarbons (PAHs), which are precursors of soot.[2−4]

Phenyl radicals and carbon monoxide coexist under sooting conditions; their interaction may affect the concentration of C_6H_5 and thus the chemistry of soot formation. The kinetics of the $C_6H_5 + CO \rightarrow C_6H_5CO$ reaction 1 is unknown, although the rate constant for the reverse process, the decomposition of the benzoyl radical, was reported by Solly and Benson[5] more than 30 years ago. In their study with the I_2-catalyzed decomposition of benzaldehyde in a narrow temperature range of 614−667 K, the first-order (high-pressure) rate constant, $k_1^\infty = 4 \times 10^{14}\exp(-14\,800/T)$ s^{-1}, was evaluated by extrapolating the rate coefficients obtained in the falloff region using assumed transition-state structure and vibrational frequencies by both Rice−Ramsperger−Kassel (RRK) and Rice−Ramsperger−Kassel−Marcus (RRKM) theories.[5] Their result was consistent with the heat of the dissociation reaction at 298 K, $\Delta H_{-1}^\circ =$ 27.5 kcal/mol, with a 2.3 kcal/mol $C_6H_5 + CO$ addition barrier. To our knowledge, no other kinetic data exist for the reaction in either direction since this early study.

In this investigation, we apply the technique of cavity ring-down spectrocopy (CRDS), which has been developed for kinetic applications in our laboratory since 1992[6−12] to measure the rate constant for the $C_6H_5 + CO$ addition reaction over the temperature range 295−500 K at 12−120 Torr pressure. To correlate our kinetic data with those of Solly and Benson,[5] we also performed quantum chemical calculations to provide the molecular and transition-state parameters for a more reliable prediction of the temperature (*T*) and pressure (*P*) effects on the rate constants for both forward and reverse directions by means of the RRKM theory.[13] The results of this investigation are reported here.

Experimental Procedure

The experimental apparatus and kinetic data acquisition by CRDS have been discussed in detail in our previous publications.[6−12] Two pulsed lasers were used for the pump and probe processes. A Lambda Physik LPX 105E excimer laser was used to photodissociate C_6H_5NO (nitrosobenzene) at 248 nm. A tunable, pulsed dye laser pumped by XeCl excimer laser (Lambda Physik FL 3002) was used for probing the C_6H_5 directly at 504.8 nm where a distinct absorption peak was known to exist.[6] Nitrosobenzene was placed on a sealed, fritted glass disk and carried into the reactor via a mixing tube with Ar as a carrier gas. The decay signal was measured with a Hamamatsu photomultiplier and acquired and averaged with a multichannel digital oscilloscope (LeCroy 9310M). The averaged signal was sent to a microcomputer for storage and further analysis. A pulse delay generator (SR DG535), interfaced with computer, was used to control the delay time between the two laser firings and the triggering of the oscilloscope. The lasers were typically operated at 4 Hz. The detailed experimental conditions, such as flow rates, pressure, and temperatures, used in the present study are presented in Table 1. The temperature of the cavity was controlled by resistive heating and measured using a J-type thermocouple placed a few millimeters below the central axis of the cavity. The amount of CO and the carrier gas were precisely measured with calibrated MKS mass flowmeters.

C_6H_5NO (Aldrich, 97%) was recrystallized using ethanol as solvent and vacuum-dried. The CO reactant was purified by passing through the silica gel trap at 180 K [to remove impurities such as $Fe(CO)_5$] and introduced into the cavity without carrier

* Corresponding author. E-mail: chemmcl@emory.edu.

† Permanent address: State Key Laboratory for Physical Chemistry of Solid Surfaces, Institute of Physical Chemistry and Department of Chemistry, Xiamen University, Xiamen, 361005, P. R. of China.

10.1021/jp993245a CCC: $19.00
Published on Web 01/21/2000

TABLE 1: Measured Rate Constants[a] and Heat of Reaction[b] for the $C_6H_5 + CO \rightarrow C_6H_5CO$ Reaction

T (K)	P (Torr)	P_{co} (Torr)	$k_1 \times 10^{-10}$	ΔH_1°
295	40	0 − 11.10	0.51 ± 0.08[c]	−24.65 ± 0.09
319	40	0 − 10.30	0.80 ± 0.12[c]	−24.67 ± 0.09
336	40	0 − 9.75	0.96 ± 0.10[c]	−24.61 ± 0.07
347	12	0 − 4.27	1.14 ± 0.22[c]	−24.65 ± 0.12
347	40	0 − 8.97	1.16 ± 0.22[c]	−24.63 ± 0.12
347	80	0 − 11.80	1.13 ± 0.16[c]	−24.59 ± 0.09
347	120	0 − 14.90	1.11 ± 0.07[c]	−24.60 ± 0.04
369	40	0 − 7.40	1.41 ± 0.64[d]	−24.56 ± 0.27
397	40	0 − 8.26	1.70 ± 0.38[d]	−24.44 ± 0.16
419	40	0 − 6.00	2.16 ± 0.37[d]	−24.45 ± 0.13
442	40	0 − 5.68	2.95 ± 0.17[d]	−24.54 ± 0.05
467	40	0 − 5.85	4.02 ± 0.70[d]	−24.66 ± 0.15
500	40	0 − 2.95	4.56 ± 2.20[d]	−24.60 ± 0.39
average				−24.59 ± 0.14

[a] Rate constants are given in units of cm^3 $mole^{-1}$ s^{-1} and their associated errors represent one standard deviations. [b] Evaluated by the third-law method (see below) given in units of kcal/mol. [c] Analyzed by eq 1. [d] Analyzed by eq 6.

gas. Ar (Specialty Gases, 99.995% UHP grade) was used to carry the vapor of nitrosobenzene into the cavity without further purification.

Data Acquisition. The CRDS method measures the decay times of injected probing photons in the absence (t_c^0) and presence (t_c) of absorbing species. Because of the high-quality resonant cavity used, the injected dye laser pulse was typically lengthened by a factor of $2-3 \times 10^3$, giving $t_c^0 \cong 20$ μs in the absence of an absorbing species, denoted by A. In the presence of the absorbing species such as C_6H_5, the photon decay time at 504.8 nm (t_c) was shortened by about 25% from that of t_c^0 immediately after photodissociation. Because the measured values of t_c and t_c^0 are much smaller than the chemical decay time of the radical, t, which depends on the concentration of the molecular reactant, the following kinetic relationship holds[6,7]

$$1/t_c = 1/t_c^0 + (cl\epsilon/nL)[A]_t \quad (1)$$

where c is the velocity of light, l is the length of the absorbing medium, ϵ is the extinction coefficient, n is the refractive index of the medium, L is the length of the cavity, and $[A]_t$ is the concentration of the absorbing species at time t. For a simple association reaction with a deep well (without the problem of redissociation), A decays exponentially with $[A]_t = [A]_0\, e^{-k't}$.

Combination with eq 1 leads to[6−12]

$$\ln(1/t_c - 1/t_c^0) = B - k't \quad (2)$$

where $B = \ln\{(cl\epsilon/nL)[A]_0\}$. The validity of eq 2 has been illustrated previously[6−12]; the equation will be used later for analysis of low-temperature data. According to eq 2, the slope of a $\ln(1/t_c - 1/t_c^0)$ vs t plot gives the first-order rate coefficient, k', for the decay of A, or the C_6H_5 radical, in the presence of a specified molecular reactant concentration, [CO]. A standard plot of k' vs [CO] provides the second-order rate constant, k_1, according to the relationship:

$$k' = k_0 + k_1[CO] \quad (3)$$

where k_0 is the first-order decay coefficient of the radical in the absence of the molecular reactant; it is a convoluted decay rate, consisting of the losses by diffusion, pumping, and recombination reactions.

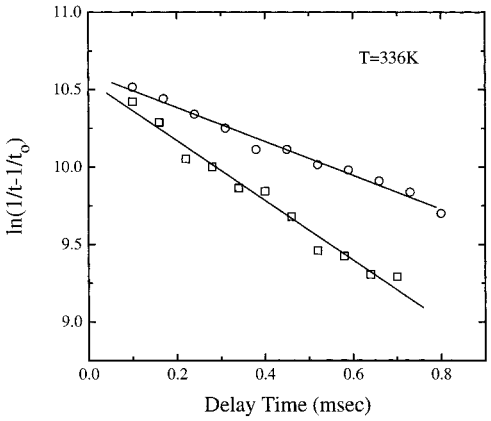

Figure 1. Typical pseudo-first-order decay plots for the $C_6H_5 + CO$ reaction under different, excess reactant concentrations in units of mol/cm^3 at 336 K. ○, $[CO] = 1.66 \times 10^{-8}$; □, $[CO] = 9.75 \times 10^{-8}$.

Equation 2 may not be valid for the $C_6H_5 + CO$ reaction at higher temperatures because of the inception of the reverse reaction (−1):

$$C_6H_5 + CO \leftrightarrow C_6H_5CO\ (1, -1)$$

In this case, the rate equation should include the reverse term:

$$dx/dt = k_1([A]_0 - x)[CO] - k_{-1}x \quad (4)$$

where $x = [A]_0 - [A]_t$, and $[A]_t$ represents the concentration of the benzoyl radical at time t. Integration of eq 4 under excess CO concentration conditions gives

$$x = (a/b)\,(1 - e^{-bt}) \quad (5)$$

where $a = k_1\,[CO][A]_0$ and $b = k_1[CO] + k_{-1}$. Combining eqs 1 and 5 leads to the following general expression for the reversible reaction:

$$1/t_c - 1/t_c^0 = k_{-1}d/b + (k_1[CO]d/b)e^{-bt} \quad (6)$$

In eq 6, $d = 1/t_c^0 - 1/t_c^0$; where t_c^0 is the photon decay time measured immediately after the photolysis of C_6H_5NO at $t = 0$. Because d is proportional to the initial concentration of C_6H_5, it is a constant for each experimental run. Equation 6 will be used to analyze data obtained at higher temperatures at which the redissociation of C_6H_5CO becomes significant.

Results and Discussion

A. Kinetics of $C_6H_5 + CO$. The rate constants for the $C_6H_5 + CO$ reaction were measured in the temperature range between 295 and 500 K at 12−120 Torr pressure with Ar as a carrier gas. Figure 1 presents typical pseudo-first-order plots for the decay of C_6H_5 at 336 K in the presence of the different amounts of CO at 40 Torr total pressure, as indicated in the caption of the figure. As shown in the figure, the data exhibit the good linear quality of the $\ln(1/t_c - 1/t_c^0)$ vs t plot as predicted by eq 1. The slope of the plot, the pseudo-first-order rate coefficient (k') of the reaction at each CO concentration, was obtained by a standard weighted least-squares analysis. At temperatures higher than 400 K the first-order decay plots in the present system become nonlinear with time t as illustrated in the inset of Figure 2. The deviation can be attributed to the regeneration of C_6H_5 by the decomposition of C_6H_5CO at higher temperatures because of the low thermal stability of the radical product, as

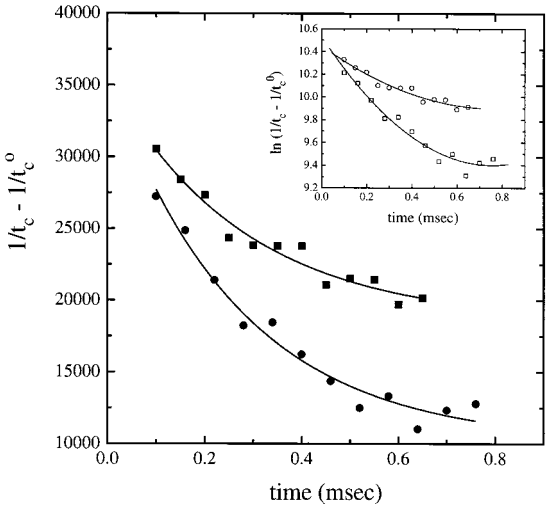

Figure 2. Typical $1/t_c - 1/t_c^0$ vs time plots at 446 K according to eq 6. Curves are least-squares fits. Inset: plots showing deviation from eq 1 for the same sets of data.

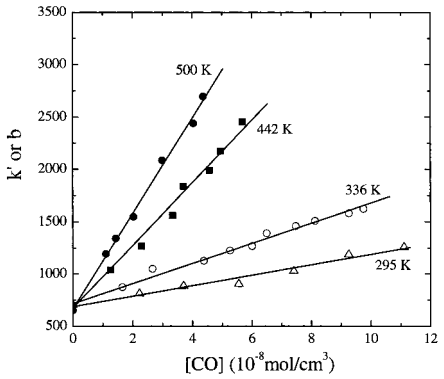

Figure 3. k' (open symbols) or b (solid symbols) vs [CO] at different temperatures. Linear least-squares fit yields the second-order rate constant k_1.

discussed in the preceding section. These nonlinear data, if analyzed with eq 1, underpredict the values of k_1 as one would expect. Accordingly, all data acquired near and above 400 K were evaluated with eq 6, which can be effectively represented by

$$1/t_c - 1/t_c^0 = c_1 + c_2\, e^{-bt} \qquad (7)$$

where c_1 and c_2 are constants for each experimental run and $b = k_1[\mathrm{CO}] + k_{-1}$ as defined before.

The nonlinear fitting of $(1/t_c - 1/t_c^0)$ against t according to eq 7, illustrated in Figure 2 by solid curves, gives values of b which vary linearly with [CO].

The second-order plots of k' or b vs [CO] are presented in Figure 3. The slopes of these plots give the bimolecular rate constants for the C_6H_5 + CO reaction. The values of k_1 evaluated for 40 Torr pressure with eqs 1 and 7 are presented in Figure 4 by circles and squares, respectively. As is evident from the figure, the values of k_1 evaluated with the two equations differ greatly above 400 K because of the redissociation reaction. The values obtained with the two methods converge at temperatures where redissociation becomes negligible.

The second-order rate constants obtained with eq 1 for $T <$ 400 K and with eq 7 for $T >$ 400 K are summarized in Table 1. A weighted least-squares analysis of these data gives rise to

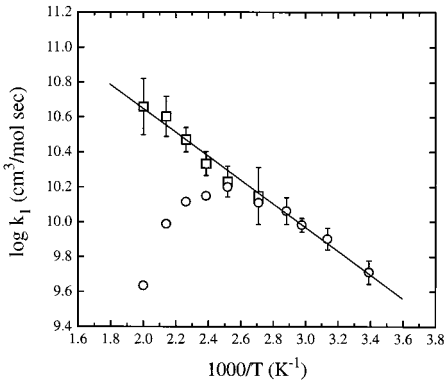

Figure 4. Arrhenius plot of k_1 at the total pressure 40 Torr. The solid line is the result of a weighted least-squares analysis. Circles, k_1 evaluated by eqs 1 and 2; squares, k_1 evaluated by eqs 7 and 2 to minimize the effect of the reverse reaction.

$$k_1 = 10^{11.93\pm0.14} \exp[(-1507 \pm 109)/T]\ \mathrm{cm^3\ mole^{-1}\ s^{-1}} \qquad (8)$$

for the temperature range 295−500 K at 40 Torr Ar pressure. The errors cited above represent two standard deviations.

We have also examined the effect of pressure on the reaction at 347 K by varying the total pressure from 12 to 120 Torr. As shown in Figure 5, the effect is negligible under the conditions studied. At higher temperatures, however, the pressure effect becomes significant as illustrated by the predicted pressure dependence presented in the inset of the figure. At the highest temperature studied, 500 K, k_1 is about 70% of the high-pressure limit. After the correction for the falloff effect with the RRKM theory to be discussed below, the high-pressure, second-order rate constant can be described by the equation:

$$k_1^{\infty} = 10^{12.17\pm0.18} \exp[(-1676 \pm 149)/T]\ \mathrm{cm^3\ mole^{-1}\ s^{-1}} \qquad (9)$$

B. Theoretical Analysis of Kinetic Data. The measured kinetic data for the C_6H_5 + CO reaction and those of Solly and Benson[5] for the reverse process have been correlated with the RRKM theory using the molecular and transition-state parameters computed by different quantum chemical methods.

Quantum Calculations. The geometries of the reactants, transition state, and product have been optimized using two different methods, MP2 and B3LYP (i.e. Becke's three-parameter nonlocal-exchange functional[14] with the nonlocal correlation functional of Lee et al.).[15] Vibrational frequencies have been used for characterization of stationary points, zero-point energy (ZPE) corrections, and RRKM calculations. In the RRKM calculations, vibrational frequencies obtained by B3LYP/6-311G(d,p) and MP2/6-31G(d,p) were scaled by 1.0[16] and 0.9434,[17] respectively. All the stationary points have been positively identified for stable species (with the number of imaginary frequencies NIMAG = 0) and transition state (with NIMAG = 1). All calculations were carried out with the Gaussian 94 program.[17]

Both MP2 and B3LYP methods predict similar structures for the ground-state C_6H_5CO radical. However, for the transition state, B3LYP gives a much longer dissociating C−C bond (2.493 Å vs 2.215 Å by MP2) and thus a much looser TS structure which predicts a considerably higher A-factor than the experimentally measured value. Its consequence will be referred to below. The calculated MP2 geometries of the C_6H_5CO and its transition state are presented in Figure 6 together with those of the CH_3CO system for comparison and further discussion on the effect of resonance stabilization on the thermochemistry of the benzoyl radical later.

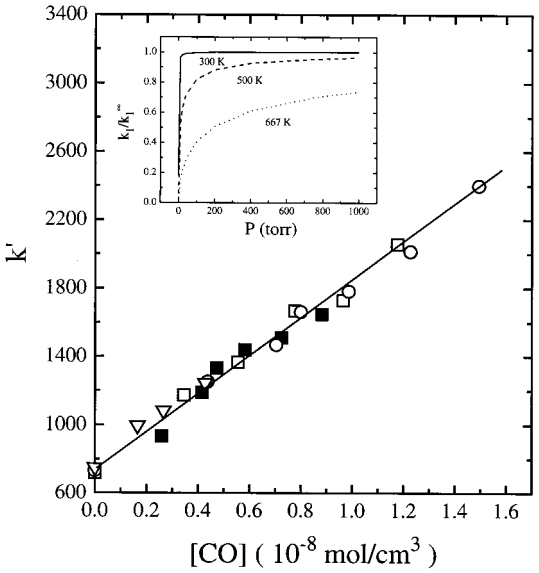

Figure 5. The pseudo-first-order decay plots for the reaction of C_6H_5 with CO obtained at different total pressures at 347 K. ▽, 12 Torr; ■, 40 Torr; □, 80 Torr; ○, 120 Torr. Inset, pressure effect on the second-order rate constant, k_1, predicted by the RRKM theory at the temperature indicated. 500 and 667 K represent the highest temperature used in this and Solly and Benson's study.[5]

Rate Constant Calculation. Because of the large size of the present system (8 heavy atoms with open shell), the heat of the reaction and the barrier for the addition process cannot be reliably predicted. To circumvent the shortcoming, we calculate k_1 by adjusting the reaction barrier using the RRKM theory with the computed geometries and vibrational frequencies of the reactants and the transition state.

In Figure 7 we compare the calculated rate constants using the molecular parameters computed with the two different methods. As illustrated in the figure, the RRKM//MP2/6-31G-(d,p) calculation with the adjusted $E_1^\circ = 2.9$ kcal/mol appears to give a better fit to experimental data than the RRKM//B3LYP/6-311G(d,p) result does with the adjusted $E_1^\circ = 4.0$ kcal/mol (in terms of both temperature dependence and the absolute value of k_1). As indicated above, the latter method predicts a looser TS with a larger A-factor which requires concomitantly a higher reaction barrier to match the theory with experiment. The 4.0-kcal/mol barrier height is greater than the experimental activation energy by 1 kcal/mol; this is not acceptable and inconsistent with TST.

Correlation with the Reverse Rate Constant. As mentioned in the Introduction, Solly and Benson[5] first reported the kinetics for the C_6H_5CO decomposition reaction using the I_2-catalyzed reaction of C_6H_5CHO at 614−667 K with pressures varying from 245 to 461 Torr. Their experimental conditions and the first-order coefficients, k_{-1} (T,P), are summarized in Table 2. Because the mixtures used contain C_6H_5CHO, I_2, HI, and the key reaction products, CO and C_6H_5ClO, we listed the averaged molecular weights ($\bar{M}$) and Lennard−Jones parameters (L−J) ($\bar{\epsilon}$ and $\bar{\sigma}$) which are required in our RRKM calculations. Both $\bar{M}$ and L−J parameters were averaged with the mole fractions of individual components. The L−J parameters of C_6H_5CHO, I_2, HI, and Ar were calculated from their critical constants (P_c, T_c, and V_c),[18] whereas those of C_6H_5CO and C_6H_5ClO were assumed to be the same as C_6H_5CHO. The L−J parameters were used for calculation of the effective collision frequencies using Troe's weak collision approximation.[19]

Table 2 summarizes the high-pressure rate constants (k_{-1}^∞) obtained by RRKM extrapolation of Solly and Benson's k_{-1} (T,P) given in the table with an adjusted barrier for the decomposition reaction (E_{-1}°). Least-squares analysis of the computed k_{-1}^∞ for each mixture using the E_{-1}° thus derived for the temperature range 500−1000 K gives the high-pressure activation energy E_{-1}^∞, which is also presented in the table.

As revealed by the results presented in the table, E_{-1}^∞ is typically greater than the decomposition barrier by about 2 kcal/mol because of the effect of temperature on the A-factor (or the partition functions of the TS). Combination of the average value of E_{-1}°, 27.3 ± 0.6 kcal/mol, evaluated from the 21 sets of Solly and Benson's data, with the forward reaction barrier, $E_1^\circ = 2.9 \pm 0.4$ kcal/mol, gives the heat of the decomposition reaction at 0 K, $\Delta H_1^\circ = 24.4 \pm 1.0$ kcal/mol.

A more reliable alternative approach to evaluate the heat of reaction is the third-law method, using the equilibrium constant and the Gibbs energy functions, $-(G_T^\circ - H_0^\circ)/T$, computed with the predicted molecular parameters for the reactants (CO and C_6H_5) and the product (C_6H_5CO). The former can be calculated by the ratio of our forward rate constant presented in Table 1 and that for the reverse reaction calculated at the same temperature and pressure with the RRKM theory, using $E_{-1}^\circ =$ 27.3 kcal/mol derived above.

In the last entry of Table 1, we list the values of ΔH_1° calculated by the third-law method; the average of the values derived by convoluting the all errors of k_1 gives $\Delta H_1^\circ = -24.6 \pm 0.1$ kcal/mol. Incorporation of the potential error from k_{-1}, as reflected by the deviation in E_{-1}° (±0.6 as shown in Table 2), we arrive at $\Delta H_1^\circ = -24.6 \pm 0.7$ kcal/mol, which is in close agreement with the value obtained by the first-law method, $\Delta H_1^\circ = E_1^\circ - E_{-1}^\circ = -24.4 \pm 1.0$ kcal/mol as presented above.

The heat of reaction evaluated from the two independent sets of kinetic data, −24.6 kcal/mol agrees closely with the theoretically predicted values, −24.6 and −27.6 kcal/mol by B3LYP/6-311G(d,p) and MP2/6-31G(d,p), respectively.

In Figure 8, we correlate the forward and reverse rate constants; the forward rate constant was converted to k_{-1}^∞ by detailed balance ($k_{-1}^\infty = k_1^\infty K_{-1}$), whereas the reverse rate constant, listed in Table 2, was extrapolated to the high-pressure limit with Solly and Benson's $k_{-1}(T,P)$ as mentioned previously. The two sets of data can be well correlated with the Arrhenius expression calculated with the RRKM theory

$$k_{-1}^\infty = 5.27 \times 10^{14} \exp(-14\,600/T)\ \mathrm{s}^{-1} \qquad (10)$$

using the averaged 0 K barrier $E_{-1}^\circ = 27.3$ kcal/mol and the molecular parameters computed by the MP2/6-31G(d,p) method.

Equation 10 is quite close to Solly and Benson's value, $k_{-1}^\infty = 4 \times 10^{14} \exp(-14\,800/T)\ \mathrm{s}^{-1}$, obtained by extrapolation with RRK (taking $s = 20$) or RRKM calculations based on assumed strong collision efficiencies, $C_6H_5CO^\ddagger$ structure and vibrational frequencies.[5]

Heat of Formation of C_6H_5CO and D_0^o (C_6H_5−CO). The heat of reaction 1, $\Delta H_1^\circ = -24.6 \pm 0.7$ kcal/mol derived above for 0 K, allows us to calculate the heat of formation of the benzoyl radical, $\Delta_f H_0^\circ = 32.5$ kcal/mol, and $\Delta_f H_{298}^\circ = 29.0$ kcal/mol with an approximate total error of ±1.5 kcal/mol, using the heats of formation of C_6H_5[20] and CO[21] cited in Table 3. Notably, the result agrees well with several reported values,[22−24] including the earlier one derived by Solly and Benson[24] given in Table 3. The lower value of the heat of formation derived by Solly and Benson, 26.1 at 298 K or 29.6 kcal/mol at 0 K, was obtained from the kinetics of the I + C_6H_5CHO = HI + C_6H_5CO reaction, $\log k_f\ (\mathrm{cm^3\ molecule^{-1}\ s^{-1}}) = (13.08 \pm 0.16) - (8536 \pm 180/T)$, assuming the activation energy for its reverse process

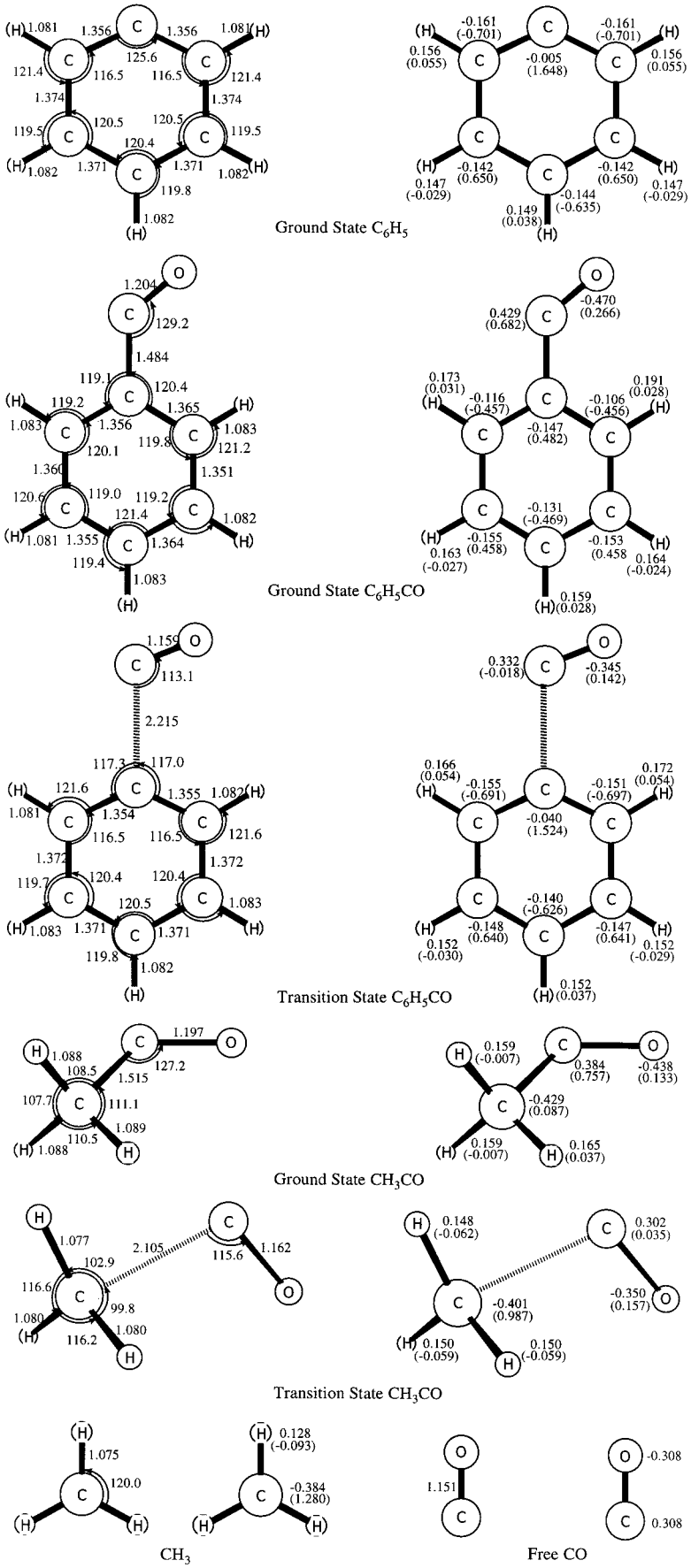

Figure 6. Optimized geometries (given in the left-hand side of the figure) and predicted atomic charge populations and spin densities (numbers in parentheses), both given in the right-hand side of the figure, for the molecular and transition states of C_6H_5CO and CH_3CO computed by the MP2/6-31(d,p) method.

TABLE 2: Extrapolation of Solly and Benson's Data (ref 5)

T (K)	P (Torr)	$\bar{M}$ (g·mol^{-1})	$\bar{\epsilon}$ (K)	$\bar{\sigma}$ (Å)	$k_{-1}(T, P)$ (10^{-4} s^{-1})	E°_{-1} (kcal mol^{-1})	k^{∞}_{1} (10^{-4} s^{-1})	E^{∞}_{-1} (kcal mol^{-1})
614.0	66.10	169.4	386	5.58	1.68	26.8	3.43	29.0
614.0	461.30	128.1	306	5.50	3.00	26.6	3.98	28.8
615.8	60.40	126.9	336	5.53	1.68	26.8	3.58	29.0
615.8	55.01	118.4	316	5.55	2.82	26.0	6.19	28.3
615.8	146.62	123.2	310	5.53	2.86	26.4	4.79	28.7
615.8	57.80	123.6	368	5.67	1.85	26.7	3.89	28.9
630.4	167.93	114.4	298	5.46	3.75	26.7	6.51	28.9
630.9	52.82	101.2	323	5.56	1.82	27.3	4.36	29.5
667.6	37.27	104.4	301	5.41	3.32	27.8	12.01	29.8
667.5	47.12	112.6	301	5.46	4.35	27.5	14.26	29.6
584.3	37.70	214.2	428	5.70	0.70	26.3	1.42	28.6
609.6	24.00	205.9	422	5.69	0.39	28.2	1.08	30.2
609.6	29.10	240.3	438	5.56	0.55	27.8	1.45	29.8
609.7	37.10	197.9	416	5.68	0.74	27.5	1.76	29.6
609.3	31.70	204.7	422	5.70	0.71	27.4	1.77	29.6
609.3	59.40	195.0	419	5.74	0.87	27.4	1.76	29.6
632.5	45.00	195.4	409	5.61	1.12	28.0	2.89	30.1
632.5	51.90	234.5	432	5.53	1.03	28.2	2.56	30.2
632.6	38.10	194.5	410	5.64	1.25	27.8	3.42	29.9
632.5	36.40	203.8	416	5.64	1.32	27.7	3.68	29.8
632.4	75.20	209.2	418	5.62	1.37	28.0	2.97	30.0
average						27.3 ± 0.6		29.4 ± 0.5

TABLE 3: Summary of Vibrational Frequencies,[a] Moments of Inertia,[a] Relative Energies,[b] and Heats of Formation of Reactants, Products, Transition States for the Reaction of $C_6H_5 + CO \rightarrow C_6H_5CO$ at the MP2/6-31G(d, p) Level of Theory[j]

			relative energies (kcal/mol)		$\Delta_f H°$ (kcal/mol)	
species	I_i (amu)	u_j (cm^{-1})	B3LYP/6-311G(d,p)	MP2/6-31G(d,p)	0 K	298.15 K
C_6H_5	277.462 311.395 588.857	441, 463, 598, 619, 669, 773, 925, 931, 974, 1025, 1038, 1053, 1057, 1076, 1130, 1179, 1202, 1296, 1494, 1506, 1735, 1786, 3079, 3088, 3108, 3113, 3113			84.3 ± 0.6[c]	81.2 ± 0.6[c]
CO	.000 32.445 32.445	1999			-27.2 ± 0.1[d]	-26.4 ± 0.1[d]
$C_6H_5 + CO$			0.0	0.0		
C_6H_5CO	318.458 1119.708 1438.166	20i[a], 192, 236, 436, 473, 504, 616, 650, 701, 808, 855, 955, 1002, 1016, 1092, 1097, 1137, 1145, 1150, 1184, 1210, 1229, 1323, 1562, 1596, 1855, 1952, 1976, 3081, 3093, 3095, 3109, 3114	−24.58	−27.55	30.3[e] 33.9 ± 1.3[f] (29.6 ± 2.0) (31.2 ± 2.6) 32.5 ± 1.5[i]	27.8[e] 30.6 ± 0.7[f] 26.1 ± 2.0[g] 27.7 ± 2.6[h] 29.0 ± 1.5[i]
C_6H_5CO (TS)	333.391 1384.273 1717.664	*388i*, 67, 112, 131, 288, 368, 496, 553, 574, 620, 684, 773, 839, 869, 904, 924, 930, 968, 997, 1096, 1097, 1228, 1250, 1384, 1405, 1458, 1481, 2007, 2963, 2971, 2981, 2988, 2991	0.73	3.33		

[a] Taken as free rotation case. [b] Includes zero-point energy correction. [c] Ref 20. [d] Ref 21. [e] G2(MP2,SVP) calculation.[23] [f] Isodesmic reaction calculation.[23] [g] Ref 24. [h] Ref 22. [i] This work. [j] All frequencies have been scaled by factor 0.9434.

to be 1 ± 1 kcal/mol. More recently, Ng and co-workers[23] obtained a higher value of the heat of formation, 33.3 ± 2.2 kcal/mol, from the photofragmentation dynamics study of acetophenone using a time-of-flight mass spectrometric technique. This result agrees most closely with our value (32.5 ± 1.5 kcal/mol) and also reasonably with that of Simoes and Griller, 31.2 ± 2.6 kcal/mol, obtained by photoacoustic calorimetry.[22]

The heat of reaction for the reverse reaction, (−1), $\Delta H^{\circ}_{-1} = 24.6$ kcal/mol, represents the bond dissociation energy $D_0{}^{o}$ (C_6H_5-CO). This energy is higher than that of the analogous process,

$$CH_3CO \rightarrow CH_3 + CO$$

by 15 kcal/mol (based on the value, $D_{298}{}^{o}$ (CH_3-CO) = 11 kcal/mol[25]). The greater strength of the >C−CO bond in the benzoyl radical could be intuitively attributed to the existence of the following resonance structures[24]:

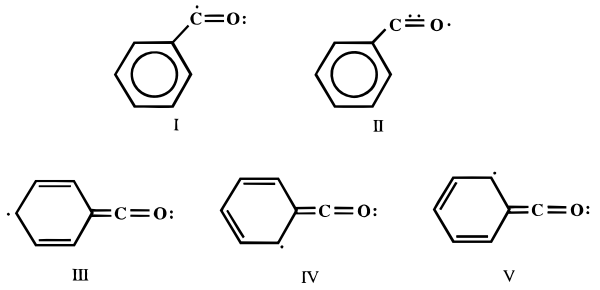

These resonance structures can lead to a higher stability for C_6H_5CO than its alkyl analogue. Solly and Benson,[24] on the other hand, favored solely a contribution from structure II shown above, with no contributions from structures III−V and thereby preserving the large resonance energy of the benzene ring.

The above-mentioned argument, however, is not fully supported by the result of our quantum calculation presented in Figure 6, in which we compare the bond lengths, atomic charge

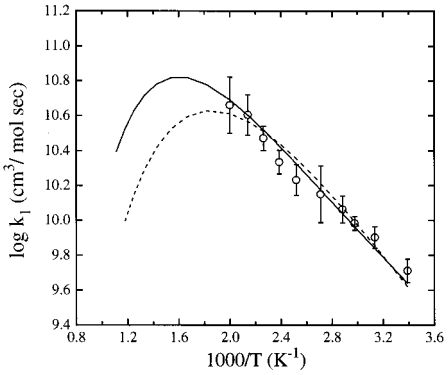

Figure 7. Comparison of the experimental and theoretically predicted results for the C_6H_5 + CO reaction at the total pressure 40 Torr. ○, experimental result (this work); solid and dashed lines, the RRKM results calculated with TS parameters obtained by using MP2/6-31G(d,p) and B3LYP/6-311G(d,p) with E_1° = 2.9 and 4.0 kcal/mol, respectively. The decrease of the predicted rate constants at higher temperatures resulted from the falloff effect.

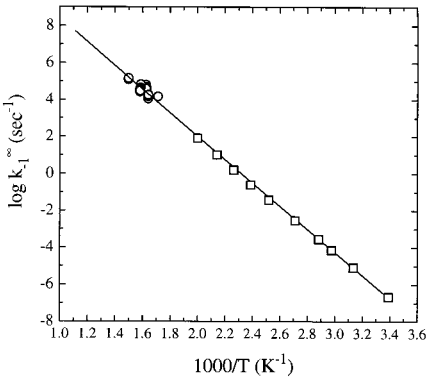

Figure 8. Correlation of Benson's data (○) for $C_6H_5CO \rightarrow C_6H_5$ + CO extrapolated to the high-pressure limit and our rate constant for C_6H_5 + CO → C_6H_5CO converted to k_1^∞ (□) with the equilibrium constant $K_{-1} = 5.41 \times 10^{24} \exp(-12\,500/T)$ cm^3/mol. Solid line, the predicted first-order rate constant by RRKM calculations (see text).

populations, and atomic spin densities of C_6H_5CO with those of CH_3CO. First of all, the dissociating C−C bond in the benzoyl radical is 1.484 Å, which is shorter than that in CH_3-CO, 1.515 Å. The corresponding C−C bond lengths in the transition states, however, are reversed, slightly longer in C_6H_5-$CO^‡$ (2.215 Å) than that in $CH_3CO^‡$ (2.105 Å), suggesting that the former is an earlier TS than the latter in the R + CO addition reactions (reflecting the greater reactivity of C_6H_5 than CH_3). The charge populations in the carbonyl group of C_6H_5CO are only slightly higher than those in CH_3CO. Similarly, the spin density at the C atom of the CO group in C_6H_5CO, 0.682, is only slightly lower than that in CH_3CO, 0.757, and the corresponding values at the O atoms, 0.266 and 0.133, respectively, are considerably smaller than what would be expected for the O atom in structure II, with a value between 1 and 2. These results indicate that all the resonance structures given above do contribute partly to the overall greater stability and thus the higher dissociation energy of the C_6H_5CO radical.

Concluding Remarks

In this study, we measured for the first time the rate constant for the association of C_6H_5 with CO by cavity ring-down spectrometry at temperatures between 295 and 500 K mostly at 40 Torr Ar pressure. The reaction was weakly pressure-independent at $T > 400$ K. Our result could be reasonably correlated with that of the reverse process reported by Solly and Benson[5] using the RRKM theory with the molecular and transition-state parameters computed by MP2/6-31G(d,p) calculations. Combination of the two sets of kinetic data yields the heat of the reaction, C_6H_5 + CO = C_6H_5CO (1), $\Delta H_1^\circ = -24.6$ kcal/mol by the third-law method. This result, combined with the known heats of formation of the reactants, gives rise to the heat of formation of the benzoyl radical, 32.5 ± 1.5 kcal/mol at 0 K.

The heat of formation of the benzoyl radical thus derived agrees reasonably with the existing data in the literature within a rather large range of experimental errors, ±3 kcal/mol. Further work apparently is needed to improve the accuracy.

Acknowledgment. The authors are grateful for the support of this work from the Basic Energy Sciences, Department of Energy, under contract no. DE-FG02-97-ER14784.

References and Notes

(1) Sawyer, R. F. *Twenty-forth Symposium (International) Combustion*; The Combustion Institute: Pittsburgh, PA, 1992; p 1423.
(2) Glassman, I. *Combustion*, 2nd ed., Academic Press: NY, 1986.
(3) Fahr, A.; Mallard, S. G.; Stein, S. E. *Twenty-first Symposium (International) on Combustion*; The Combustion Institute: Pittsburgh, PA, 1986; p 825.
(4) Fahr, A.; Stein, S. E. *Twenty-second Symposium (International) on Combustion*; The Combustion Institute: Pittsburgh, PA, 1988; p 1023.
(5) Solly, R. K.; Benson, S. W. *J. Am. Chem. Soc*. **1971**, *93*, 2127.
(6) Yu, T.; Lin, M. C. *J. Am. Chem. Soc*. **1993**, *115*, 4371.
(7) Lin, M. C.; Yu, T. *Int. J. Chem. Kinet*. **1993**, *25*, 875.
(8) Yu, T.; Lin, M. C. *J. Phys. Chem*. **1995**, *99*, 8599.
(9) Yu, T.; Lin, M. C. *J. Am. Chem. Soc*. **1994**, *116*, 9571.
(10) Yu, T.; Lin, M. C. *Combust. Flame* **1995**, *100*, 169.
(11) Park, J.; Chakraborty, D.; Lin, M. C. *J. Phys. Chem*. **1999**, *103*, 4003.
(12) Park, J.; Lin, M. C. *Cavity-Ring-Down Spectrometry: A New Technique for Trace Absorption Measurements*; ACS Publication Series 720; Washington, DC, 1999, p 196.
(13) Diau, E. W. G.; Lin M. C. *J. Phys. Chem*. **1995**, *99*, 6589.
(14) Becke, A. D. *J. Chem. Phys.* **1992**, *96*, 2155; *97*, 9173; **1993**, *98*, 5648.
(15) Lee, C.; Yang, W.; Parr, R. G. *Phys. Rev.* **1988**, *B37*, 785.
(16) Mebel, A. M.; Morokuma, K.; Lin, M. C. *J. Chem. Phys.* **1995**, *103*, 7414.
(17) Frisch, M. J.; Trucks, G. W.; Schlegel, H. B. W.; Gill, P. M.; Johnson, B. G.; Robb, M. A.; Cheeseman, J. R.; Keith, T.; Petersson, G. A.; Montgomery, J. A.; Raghavachari, K.; Al-Laham, M. A.; Zakrzewski, V. G.; Ortiz, J. V.; Foresman, J. B.; Cioslowski, J.; Stefanov, B. B.; Nanayakkara, A.; Challacombe, M.; Peng, C. Y.; Ayala, P. Y.; Chen, W.; Wong, M. W.; Andres, J. L.; Replogle, E. S.; Gomperts, R.; Martin, R. L.; Fox, D. J.; Binkley, J. S.; Defrees, D. J.; Baker, J.; Stewart, J. P.; Head-Gordon, M.; Gonzalez, C.; Pople, J. A. *Gaussian 94*, Revision D.3 ed.; Department of Chemistry, Carnegie Mellon University, Pittsburgh, PA, 1995.
(18) Stiel, L. I.; Thodos, G. *J. Chem. Eng. Data* **1962**, *7*, 234.
(19) Troe, J. *J. Chem. Phys*. **1977**, *66*, 4745.
(20) Davico, G. E.; Bierbaum, V. M.; DePuy, C. H.; Ellison, G. B.; Squires, R. R. *J. Am. Chem. Soc.* **1995**, *117*, 2590.
(21) Chase, M. W., Jr.; Davles, C. A.; Downey, J. R., Jr.; Frurip, D. J.; McDonald, R. A.; Syverud, A. N. JANAF Thermochemical Tables. *J. Phys. Chem. Ref. Data* **1985**, *14* (Suppl. 1).
(22) Simoes, J. A. M.; Griller, D. *Chem. Phys. Lett.* **1989**, *158*, 175.
(23) Zhao, H.-Q.; Cheung, Y.-S.; Liao, C.-L.; Ng, C. Y.; Li, W.-K. *J. Chem. Phys.* **1997**, *107*, 7230.
(24) Solly, R. K.; Benson, S. W. *J. Am. Chem. Soc*. **1971**, *93*, 1592.
(25) *CRC Handbook of Chemistry of Physics*, 78th ed.; Lide, D. R., Jr., Ed.; CRC Press: Boca Raton, 1997−98.